

Love-wave dispersion from collocated measurements of rotations and translations

Suryanto, W.¹, H. Igel¹, A. Cochard^{1,2}, J. Wassermann¹, U. Schreiber³, A. Velikoseltsev³

5 ¹*Department of Earth and Environmental Sciences, Geophysics Section, Ludwig-Maximilians Universität München, Theresienstr 41, D-80333, Germany.*

²*now at: Ecole et Observatoire des Sciences de la Terre, Institut de Physique du Globe, 5 rue René Descartes, F-Strasbourg Cedex, France*

10 ³*Forschungseinrichtung Satellitengeodäsie, Technical University of Munich, Fundamentalstation Wettzell, Sackenriederstr. 25, D-93444 Kötzting, Germany.*

Recently, ring-laser based measurements of rotational ground motions (around a vertical axis) were shown to be consistent in phase and amplitude with collocated recordings of translations with standard broadband seismometers. The consistency is based on the theoretical relation between transverse acceleration and rotation rate: Assuming plane wave propagation they should be in phase and their amplitude ratio proportional to horizontal phase velocity. This suggests that collocated measurements of translations and rotations allow the determination of Love wave dispersion curves, information that is otherwise only accessible through seismic array observations or additional strain measurements. In this study, we present a novel approach to estimate frequency-dependent horizontal phase velocities by averaging spectral ratios of translations and rotations from several earthquakes of varying epicentral distances and frequency content. Comparison with theoretical Love-wave dispersion for a spherically symmetric Earth model suggests that the point measurements capture well the expected dispersive behavior. Such point-measurements with additional rotation sensors may prove to be useful for very sparse or single-station networks (e.g. in oceanography or planetary seismology) once appropriate sensors are available.

Keywords: surface waves, seismic rotations, phase velocity, Love wave dispersion

Introduction

30 The determination of frequency-dependent surface-wave phase velocities has
for a long time been one of the most important tools to determine 3-D seismic
velocity structure on regional and global scales (e.g., Nataf et al., 1984, 1986; Snieder,
1988ab, and many others). On small scales, near-surface low-velocity structures –
crucial for the estimation of hazard-relevant site effects – can be determined using
35 ambient noise measurements (e.g., Milana et al., 1996, Kind et al., 2005). Recently, it
was shown that Rayleigh-wave dispersion curves can be derived by correlating long
time series of ambient noise (micro-seismicity) and that the velocity structure thus
derived can be used to image 3-D structures (Campillo and Paul, 2003; Shapiro and
Campillo, 2004; Shapiro et al., 2005). The aforementioned techniques require
40 observations from seismic arrays to recover frequency-dependent propagation times
(and thus phase velocities) across the array in the direction of propagation.

Standard seismic observations are restricted to three components of translations,
despite the fact that the recovery of the complete motion requires the observation of
three additional components of rotations and six components of strain (e.g., Aki and
45 Richards, 2002; Trifunac and Todorovska, 2001). In the past years, rotation sensor
technology has been improving in a way that may allow the development of routine
sensors for three additional rotational motion components useful for seismological
purposes (e.g., Schreiber et al., 2005, 2006). Recent observations of local, regional
and global wavefields using ring laser technology showed that the rotational
50 measurements are fully consistent with collocated observations of translations (e.g.,
Igel et al., 2005; Cochard et al., 2006; Igel et al., 2006) following earlier observations
of earthquake-induced rotational motions (McLeod et al., 1998; Pancha et al., 2000).

Further confirmation of accurate measurements of the new observational component using ring laser technology came through comparison with rotational motions derived from seismic array data (Suryanto et al., 2006) using a classical approach (e.g., Spudich et al. (1995)). A temporary array was installed around the ring laser instrument and direct and array-derived rotations compared for an event with high signal-to-noise ratio. The high correlation-coefficient (0.93) and almost identical amplitudes for the two independent rotation measurements observed with entirely different physical principles further indicate that the ring laser indeed measures the rotational motions accurately in a wide frequency range.

A simple relationship between transverse acceleration and rotation rate (around a vertical axis) shows that both signals should be in phase and their ratio proportional to horizontal phase velocity. Igel et al. (2005) and Cochard et al. (2006) exploited this relationship to estimate horizontal phase velocities in sliding time windows along the observed time series. Comparison with synthetic traces (rotations and translations) and phase velocities determined in the same way showed good agreement with the observations. These initial results suggested that the determination of Love-wave dispersion curves (and thus information on local 1-D shear velocity structure) may be possible. It is worth noting that a similar relationship between strain and displacements can be used to determine horizontal phase velocities (e.g., Mikumo and Aki, (1964), Gomberg and Agnew (1996)).

In this study we present a novel method for the determination of Love-wave phase velocities based on collocated measurements of translations (standard broadband seismometer) and rotations around a vertical axis (observed by a ring laser). Instead of determining phase velocities in the time domain (Igel et al., 2005; Cochard et al., 2006), we average spectral ratios of several earthquakes which allows

us to directly determine frequency dependent Love-wave phase velocities and compare them with theoretical predictions for spherically symmetric Earth models.

80 The results are supported by applying the same processing steps to complete 3-D synthetic seismograms for some of the observed events.

Observations and data processing

We use translation data from station Wettzell (WET) of the German Regional Seismic Network (GRSN) located in Southern Germany (12°52'44"E, 49°08'39"N).

85 The station is equipped with an STS-2 broadband instrument with a flat response to ground velocity from 8.33 mHz (120 s) to 50 Hz. The data with a sampling rate of 80 Hz are corrected for instrument response, rotated into a local radial-transverse system, and differentiated to obtain transverse acceleration. The rotational data are measured by a ring laser instrument, called "G", consisting of a He-Ne gas laser with an
90 ultrahigh vacuum quality cavity enclosing an area of 16 m². The vertical component of rotation rate is recorded by this instrument with a sampling rate of 4 Hz. The instrumental sensitivity of ring lasers is limited by the scale factor and quantum noise processes. For the G ring laser rotation rates as small as 10⁻¹⁰ rad/s/ $\sqrt{\text{Hz}}$ can be observed (Schreiber et al., 2003). Further information on the ring laser instrument is
95 given in Schreiber et al. (2005). The ring laser is mounted horizontally in the Geodetic Fundamentalstation Wettzell (about 250 m from the STS-2 seismometer). Given the frequency range (i.e., spatial wavelengths) considered below, we treat the two observations (rotations and translations) as collocated.

From a growing event database with translations and rotations (see Igel et al.,
100 2006) we use several regional and global earthquakes in 2003 and 2004 with $M > 5.7$, listed in Table 1.

Examples of phase determination in the time-domain

We first illustrate the possibility of deriving phase velocities using the time-domain approach pursued by Igel et al. (2005, 2006). In Figure 1a+b, time series of transverse acceleration (gray) and rotation rate (black) are shown for two events, the M6.3, Greece, 14 August, 2003, and the M6.7, Siberia, 1 October, 2003, respectively. The almost identical waveform fit between rotations and translations in both cases illustrate that the assumption of plane wave propagation is appropriate and that information on the horizontal phase velocity should be contained in the ratio between transverse acceleration and rotation rate.

An appropriate measure of the fit between two presumably synchronous signals is the zero-lag normalized cross-correlation coefficient. We quantify the time-dependent similarity between rotation rate and transverse acceleration by sliding a time-window (10 s) along the time series and calculate the cross-correlation coefficient that is defined between 0 (no similarity) and 1 (perfect match). If the quality of the waveform fit in a given time window is above a threshold (0.95) we estimate a horizontal phase velocity for this time window by finding the best-fitting velocity in a least-squares sense, as well as the associated variance. These phase velocities and the associated uncertainties are shown for two particular earthquakes in the bottom plots of Figures 1a and 1b for time windows containing the fundamental Love-waves mode. In both cases, the estimated phase velocities are within the expected range of fundamental mode Love-wave phase velocities for spherically symmetric Earth models (3-5 km/s). However, the time-domain representation makes it difficult to extract the frequency dependent behavior of Love waves. Therefore, we introduce an approach in which the phase velocities are directly estimated in the frequency domain.

Love wave dispersion

The results above and those reported by Igel et al. (2006) and Cochard et al. (2006) indeed suggest that it should be possible to determine the phase velocities as a function of frequency (dispersion) by calculating the spectral ratios of transverse acceleration and rotation rate for time windows containing the Love-wave trains. For this purpose, the rotation rate is interpolated to the same sampling points as the transverse acceleration and the Love wave train time window isolated and attenuated at the edges with a Gaussian function. Both time series are transformed into the Fourier domain and the ratio of the spectra of rotations () and transverse acceleration $a_T(\omega)$ leads to the frequency-dependent phase velocities $c(\omega)$

$$\frac{a_T(\omega)}{\Omega(\omega)} = -2c(\omega). \quad (1)$$

Because of the oscillatory nature of the individual spectra and spectral ratios we average the ratios from several events assuming that the resulting phase velocities are representative of the same subsurface volume. In addition, we smooth the ratios along the frequency axis using a Savitzky-Golay filter, a low pass filter also known as least square smoothing filter or DISPO (digital smoothing polynomial). The filter is defined as a weighted moving average with weights given as a polynomial of a certain degree; in this case we use degree two (Press et al., 2002).

We first test the methodology presented above on complete synthetic seismograms (rotations and translations) calculated for one regional (Gibraltar) and two global (Hokkaido and Papua) events using the spectral-element method (Komatitsch and Tromp, 2002a,b) employing a recent 3-D tomographic model (Ritsema and Van Heijst, 2000) and the crust model by Bassin et al. (2000). The sources are modeled as point shear dislocations with source properties from the Harvard Catalogue [<http://www.seismology.harvard.edu/>]. The resulting spectral

ratios were averaged and processed as described above. The frequency-dependent phase velocities are shown in Figure 2 as Gaussians with mean value and variance for each period. We superimpose theoretical predictions of Love-wave dispersion curves for the spherically symmetric ak135 Earth model (Kennett et al., 1995) for the fundamental and the first three higher-order modes. Despite the small number of events the estimated Love-wave phase velocities seem to capture well those predicted for the fundamental modes in a spherically symmetric Earth model. The uncertainties decrease with increasing period. In the frequency (period) window considered, the largest deviation from the predicted values are 6.1% (at period 20s).

We calculate stacked spectral ratios for the regional (Greece, Turkey, Gibraltar, Algeria) and global (all other) events listed in Table 1. The results are presented in Figure 3 in the same way as the synthetic data shown in Figure 2. Except in the period range around 10 s, the Love-wave phase velocities determined by the spectral ratios are close to the predicted values. The increase in phase velocities towards longer periods is well captured by the stacked global events, with almost constant uncertainty with period. The maximum deviations of the mean values are about 5.8% (at period 100 s). The reasons for any discrepancies may be 3-D heterogeneity, anisotropy, non-planar wavefronts, deviations from the great circle paths, or uncertainties in the observations of translations and rotations (e.g., site effects). Fully understand these potential sources of discrepancies will require a larger database, comparison with array-derived Love-wave dispersion curves and systematic synthetic studies.

Conclusions

The aim of this study was to present a novel methodology to derive Love-wave dispersion curves with point measurements of rotations (around a vertical axis) and translations. Frequency-dependent phase velocities are estimated by calculating the

ratio between the spectra of transverse acceleration and rotation rate by stacking the ratios of several events. This approach was applied to 3-D synthetic data sets and several regional and global events observed by the collocated ring laser instrument measuring the rotation rate around a vertical axis and a standard broadband sensor located at Wettzell, SE-Germany.

Both synthetic and observed dispersion curves match well those predicted for the fundamental mode Love-waves. This indicates that plane-wave theory is appropriate and that the assumption of fundamental mode Love-wave propagation is approximately fulfilled, or that the energy of higher-mode Love waves in the time-windows considered is low. The purpose of this study was primarily to illustrate the concept and show a first application to real observations. Love-wave dispersion curves can be used to derive local 1-D velocity structure and are therefore an important intermediate result for tomographic inversions. Whether the accuracy of the dispersion curves derived with the approach presented here is enough for tomographic purposes remains to be evaluated. We intend to investigate these issues by systematic synthetic studies and analysis of a larger event database. Nevertheless, the results shown here indicate that through additional measurements of accurate rotational signals, wavefield information is accessible that otherwise requires seismic array data. This may be of use when arrays are very sparse or consist of only one station (e.g., oceanography or planetary seismology). However, to make this methodology practically useful for seismology will require the development of an appropriate high-resolution six-component broadband sensor. Efforts are underway to coordinate such developments on an international scale (Evans et al., 2006).

200 **Acknowledgements**

This work is supported by the German Ministry of Research and Education (BMBF-Geotechnologien) and German Research Foundation. W.S. was supported by the German Academic Exchange Service (IQN-Georisk), and by the Graduate program THESIS funded by the Bavarian Government. We are grateful to J. Tromp and D. 205 Komatitsch for providing their Spectral Element Method code. The theoretical Love wave dispersion curve was calculated using the program *lmtor* provided by Wolfgang Friederich (available through the SPICE library, www.spice-rtn.org).

References

- 210 Aki, K. and P. Richards, 2002. Quantitative Seismology, 2nd Edition, University
Science Books.
- Bassin, C., G. Laske, and G. Masters, 2000. The Current Limits of Resolution for
Surface Wave Tomography in North America, EOS Transactions, AGU 81,
F897.
- 215 Campillo, M., and A. Paul, 2003. Long range correlations in the diffuse seismic coda,
Science, 299, 547-549.
- Cochard, A., H. Igel, A. Flaws, B. Schuberth, J. Wassermann, and W. Suryanto, 2006.
Rotational motions in seismology: theory, observation, simulation, in
Teisseyre et al., editor, Earthquake source asymmetry, structural media and
rotation effects. Springer Verlag, 391-412.
- 220 Evans J.R., A. Cochard, V. Graizer, B.-S. Huang, K. W. Hudnut, C. R. Hutt, H. Igel,
W.H.K. Lee, C.-C. Liu, R. Nigbor, E. Safak, W.U. Savage, U. Schreiber,
M. Trifunac, J. Wassermann, and C.-F. Wu, 2006. A workshop on rotational
ground motion, Seismol. Res. Lett., submitted.
- Gomberg, J., and Agnew, D., 1996. The accuracy of seismic estimates of dynamic
225 strains: An evaluation using strainmeter and seismometer data from Pinon flat
Observatory, California, Bull. Seismol. Soc. Am., 86, pp. 212-220.
- Igel, H., Cochard., A., Wassermann, J., Flaws., A., Schreiber, U., Velikoseltsev, A.,
Nguyen, P. D., 2006. Broadband Observations of Earthquake Induced
Rotational Ground Motions, Geophys. J. Int., (in press).
- 230 Igel, H., U. Schreiber, A. Flaws, B. Schuberth, A. Velikoseltsev, and A. Cochard,
2005. Rotational motions induced by the M 8.1 Tokachi-Oki earthquake,
September 25, 2003, Geophys. Res. Lett., 32, L08309.

- Kennett, B.L.N. Engdahl, E.R. and Buland R., 1995. Constraints on seismic velocities in the Earth from travel times, *Geophys J. Int.*, 122, 108-124
- 235 Kind, F., Fäh, D., and Giardini, D., 2005. Array measurements of S-wave velocities from ambient vibrations, *Geophys. J. Int.*, 160, pp. 114-126.
- Komatitsch, D., and J. Tromp, 2002a. Spectral-element simulations of global seismic wave propagation, Part I: Validation. *Geophys. J. Int.*, 149, 390-412.
- Komatitsch, D., and J. Tromp, 2002b. Spectral-element simulations of global seismic wave propagation, Part II: 3-D models, oceans, rotation, and gravity. *Geophys.*
240 *J. Int.*, 150, 303-318.
- McLeod, D. P., G. E Stedman, T. H. Webb and U. Schreiber, 1998. Comparison of standard and ring laser rotational seismograms, *Bull. Seismol. Soc. Am.*, 88, 1495-1503.
- 245 Mikumo, T., and K. Aki, 1964. Determination of local phase velocity by intercomparison of seismograms from strain and pendulum instruments, *J. Geophys. Res.*, 69, 721-731.
- Milana G., Barba, S., del Pezzo, E., Zambonelli, E., 1996. Site response from ambient noise measurements: new perspectives from an array study in Central Italy,
250 *Bull. Seis. Soc. Amer.*, 86, 320-328.
- Nataf, H.-C., I. Nakanishi, and D.L. Anderson, 1984. Anisotropy and shear velocity heterogeneities in the upper mantle, *Geophys. Res. Lett.*, 11, 109-112.
- Nataf, H.-C., Nakanishi, and D.L. Anderson, 1986. Measurement of mantle wave velocities and inversion for lateral heterogeneity and anisotropy, III. Inversion,
255 *J. Geophys. Res.*, 91, 7261-7307.

- Pancha, A., T. H. Webb, G.E. Stedman, P. McLeod and U. Schreiber, 2000. Ring laser detection of rotations from teleseismic waves, *Geophys. Res. Lett.*, 27, 3553-3556.
- Press, W. H., Teukolsky, S. A., Vetterling, W. T., and Flannery, B. P., 2002. Numerical Recipes, Cambridge University Press, pp. 650-655.
- Ritsema, J., and H. J. Van Heijst, 2000. Seismic imaging of structural heterogeneity in Earth's mantle: Evidence for large-scale mantle flow, *Science Progress*, 83, 243-259.
- Schreiber, K. U., A. Velikosevtsev, G. E. Stedman, R. B. Hurst, and T. Klügel, 2003. New applications of very large ring lasers, in *Symposium Gyro Technology*, edited by H. Sorg, 80– 87.
- Schreiber, K.U., H. Igel, A. Cochard, A. Velikosevtsev, A. Flaws, B. Schuberth, W. Drewitz, and F. Müller, 2005. The GEOsensor project: rotations - a new observable for seismology. In Rummel et al., editor, *Geotechnologies*, Springer Verlag.
- Schreiber, U., G.E. Stedman, H. Igel, and A. Flaws, 2006. Ring laser gyroscopes as rotation sensors for seismic wave studies. In "Earthquake source asymmetry, structural media and rotation effects" eds. Teisseyre et al., Springer Verlag, 377-390.
- Shapiro, N. M., and Campillo, M., 2004. Emergence of broadband Rayleigh waves from correlations of the ambient seismic noise, *Geophys. Res. Lett.*, 31, L07614, doi:10.1029/2004GL019491.
- Shapiro, N.M., M. Campillo, L. Stehly, M.H. Ritzwoller, 2005. High-resolution surface wave tomography from ambient seismic noise, *Science*, 307, 1615-1618.

- Snieder, R., 1988a. Large scale waveform inversion of surface waves for lateral heterogeneity, 1, Theory and numerical examples, *J. Geophys. Res.*, 93, 12055-12065.
- 285 Snieder, R., 1988b. Large scale waveform inversion of surface waves for lateral heterogeneity, 2, application to surface waves in Europe and the Mediterranean, *J. Geophys. Res.*, 93, 12067-12080.
- Spudich, P., L. K. Steck, M. Hellweg, J. B. Fletcher, and L. M. Baker, 1995. Transient stresses at Parkfield, California, produced by the M7.4 Landers earthquake of June 28, 1992: Observations from the UPSAR dense seismograph array. *J.*
290 *Geophys. Res.*, 100, 675-690.
- Suryanto, W., Igel, H., Wassermann, J., Cochard, A., Vollmer, D., Scherbaum, F., Schuberth, B., Schreiber, U., Velikoseltsev, A., 2006. First comparison of array-derived rotational ground motions with direct ring laser measurements, *BSSA* (in press).
- 295 Trifunac, M.D., and M. I. Todorovska (2001). A note on the useable dynamic range of accelerographs recording translation. *Soil Dyn. and Earth. Eng.*, **21**, 275-286.

Table 1. Parameters of the earthquakes used in this study.

Date	Time (UTC)	Lon.	Lat.	Magnitude	Location
21/05/03	18:44:19	003.71E	36.90N	6.8	Northern Algeria
26/05/03	09:24:32	141.45E	38.90N	7.0	Honshu, Japan
06/07/03	19:10:33	026.07E	40.34N	5.7	Turkey
14/08/03	05:14:55	020.74 E	39:19N	6.3	Greece
25/09/03	19:50:06	143.90E	41.77N	8.3	Hokkaido, Japan
27/09/03	18:52:53	087.69E	50.06N	6.6	Southern Siberia
01/10/03	01:03:25	087.68E	50.22N	6.7	Southern Siberia
05/02/04	21:05:24	135.49E	03.58S	7.0	Irian Jaya, Indonesia
27/02/04	02:27:46	003.96W	35.23N	6.3	Gibraltar

300

Figure Captions

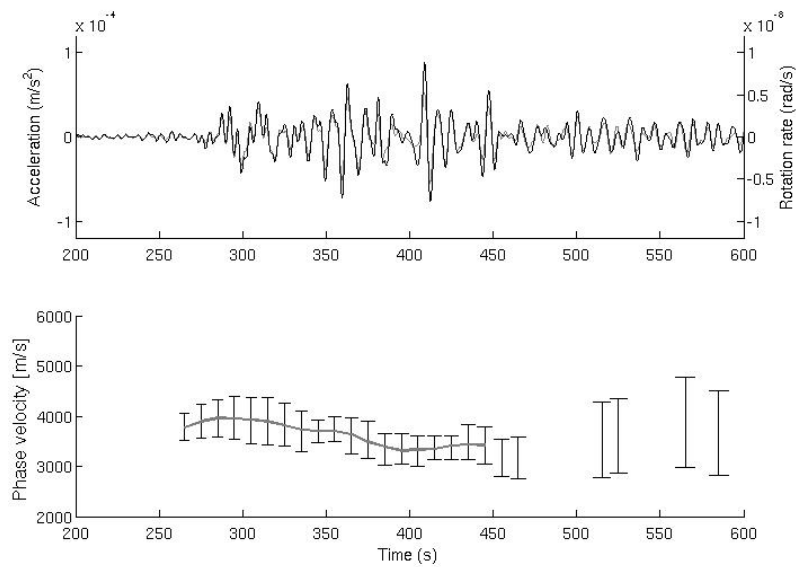
305 **Figure 1. a:** Upper trace: Transverse acceleration (gray, left axis) and rotation rate about the vertical axis (black, right axis) for the Greece event, M6.3, 14 August 2003. Bottom trace: Best-fitting horizontal phase velocities as a function of time in a 10 s sliding window. **b:** Same for the Siberia event, M6.7, 1 October 2003.

310 **Figure 2.** Frequency-dependent Love wave phase velocities from spectral ratios of synthetic seismograms calculated for the Gibraltar, Papua and Hokkaido events (see text for details) shown as mean values with variances as Gaussian uncertainties. The dashed lines indicate the theoretical fundamental- (lowest dashed line) and higher-mode Love-waves phase velocities (upper dashed lines) obtained for the ak135 Earth
315 model.

Figure 3. Love waves phase velocities derived from observed data shown as mean values (black) and associated uncertainties using grey shading (see text for details) for all event listed in Table 1. The dashed lines indicate fundamental- and higher-mode
320 Love-waves phase velocities obtained for the ak135 Earth model.

325

a



b

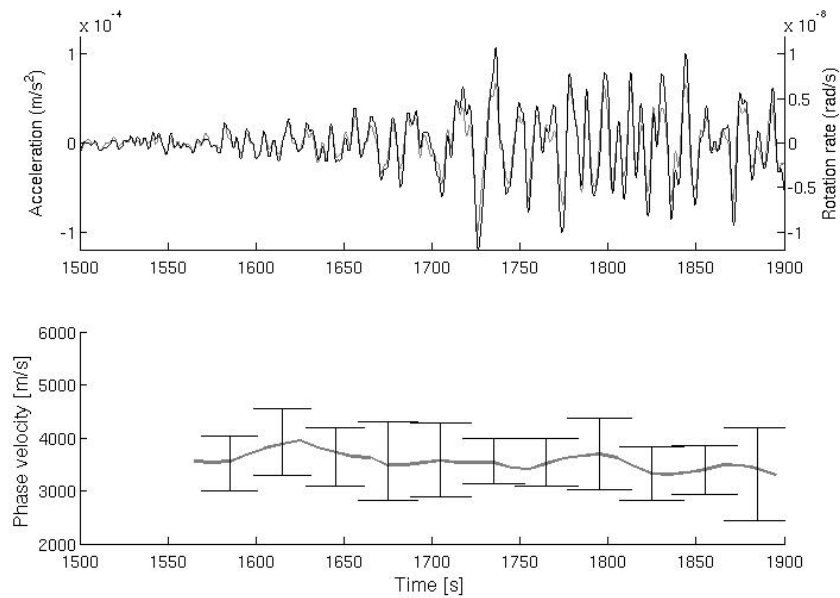


Figure 1. a: Upper trace: Transverse acceleration (gray, left axis) and rotation rate
330 about the vertical axis (black, right axis) for the Greece event, M6.3, 14 August 2003.
Bottom trace: Best-fitting horizontal phase velocities as a function of time in a 10 s
sliding window. **b:** Same for the Siberia event, M6.7, 1 October 2003.

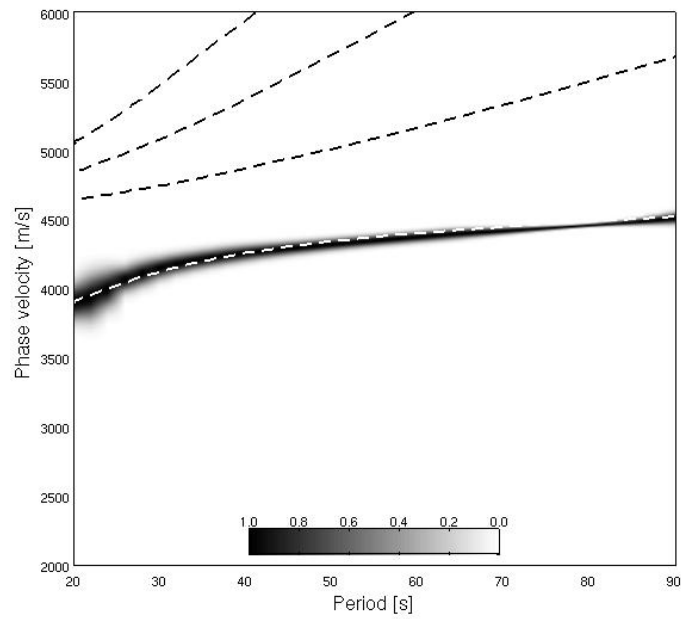


Figure 2. Frequency-dependent Love wave phase velocities from spectral ratios of
 335 synthetic seismograms calculated for the Gibraltar, Papua and Hokkaido events (see
 text for details) shown as mean values with variances as Gaussian uncertainties. The
 dashed lines indicate the theoretical fundamental- (lowest dashed line) and higher-
 mode Love-waves phase velocities (upper dashed lines) obtained for the ak135 Earth
 model.

340

345

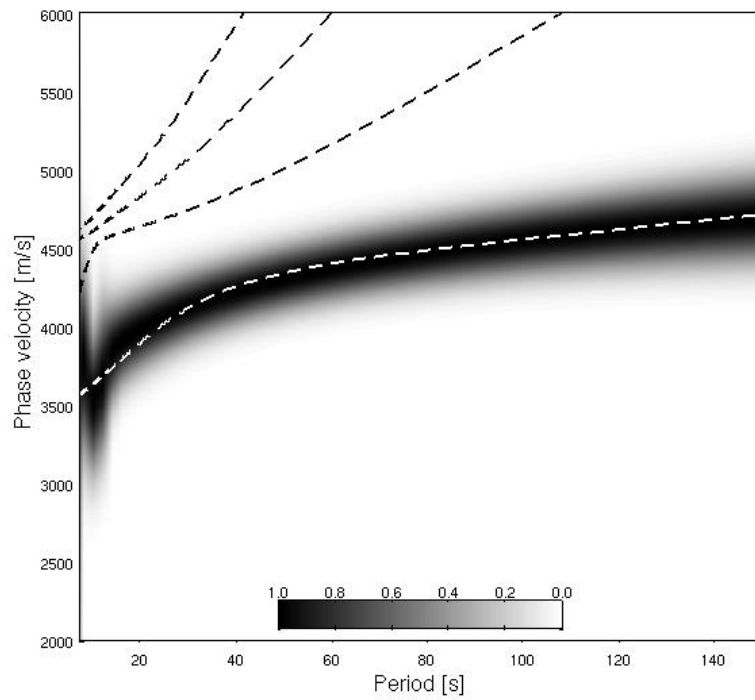


Figure 3. Love waves phase velocities derived from observed data shown as mean values (black) and associated uncertainties using grey shading (see text for details) for all event listed in Table 1. The dashed lines indicate fundamental- and higher-mode Love-waves phase velocities obtained for the ak135 Earth model.